ELSEVIER

Journal of Alloys and Compounds 311 (2000) 265–269

Journal of ALLOYS AND COMPOUNDS

www.elsevier.com/locate/jallcom

Strength and electrical conductivity of Cu–9Fe–1.2Co filamentary microcomposite wires

J.S. Song, S.I. Hong*

Department of Metallurgical Engineering, Chungnam National University, Taedok Science Town, Taejon 305-764, South Korea

Received 31 January 2000; accepted 16 June 2000

Abstract

The strength and conductivity of drawn Cu–9Fe–1.2Co microcomposite wires combined with intermediate heat treatments have been investigated. During cold working the primary and secondary dendrite arms are aligned along the drawing direction and elongated into filaments. The strengthening in Cu–Fe–Co microcomposites results from the presence of the aligned Fe–Co filaments and correlates with the fineness of the microstructural scale. The predicted strength using the Hall–Petch equation is 789 MPa, which is in reasonably good agreement with the observed strength (855 MPa). The increase of conductivity in Cu–Fe–Co after intermediate heat treatments at 450°C is attributed to the precipitation of Fe and Co atoms which were dissolved during heavy deformation processing. The tensile strength/electrical combination of 855 MPa/53.3% IACS was achieved in Cu–9Fe–1.2Co microcomposite at the cold drawing strain η=6.2.

Keywords: Transition metal alloys; Conductivity; Mechanical properties; Microstructure

1. Introduction

Microcomposites fabricated by mechanical working of ductile two-phase mixtures prepared by various techniques have been the subject of considerable research [1–6]. Tensile strengths greater than those predicted by a rule of mixtures are observed in heavily cold worked microcomposites. The tensile strengths of deformation processed microcomposites have been shown to correlate with filament spacings, leading to a Hall–Petch type relationship [3]. Spitzig et al. [3] showed that the strength of heavily cold-worked Cu–Nb microcomposite wires increased as the spacing between filaments decreased. The particularly attractive feature of these microcomposites is the combination of high strength plus high electrical and thermal conductivity [1–6]. Since the solid solubility of alloying element in Cu matrix for these microcomposites is quite small, the conductivity of the copper is not substantially reduced by the addition of alloying elements. It has been demonstrated that the similar mechanical properties were observed in other deformation processed microcomposites such as Cu–Cr, Cu–Ta and Cu–Fe [7].

The Cu–Fe system is of particular interest because of the relatively low cost of iron compared to the other possible insoluble b.c.c. phase. However, the relatively high solubility of iron in copper at high temperatures in Cu–Fe system, coupled with the slow kinetics of iron precipitation at low temperatures [8,9] is known to reduce the electrical conductivity. For this reason studies aimed at optimizing strength and conductivity have employed thermal/mechanical treatments [8,9]. Previous studies have been mostly directly to binary Cu–Fe microcomposites containing over 15 vol.% Fe [1,8,9]. With the reduction of Fe content, the conductivity is expected to increase at the expense of the strength, which could result in Cu–Fe microcomposites with favorable mechanical and electrical properties. In this study, the structure–property relationship in thermo-mechanically processed Cu–9Fe–1.2Co microcomposites was examined.

2. Experimental

Billet of Cu–9wt.%Fe–1.2wt.%Co was prepared by induction melting in air. The alloy was melt in a magnesia crucible and cast into a steel mold maintained at 200°C. The melt was deoxidized with the addition of Li-containing deoxidizer. Cylindrical billets were about 60 mm in diameter and about 112 mm in length. Extrusion of

*Corresponding author.

E-mail address: sihong@hanbat.chungnam.ac.kr (S.I. Hong).

0925-8388/00/$ – see front matter
PII: S0925-8388(00)01087-2

cylindrical billets was carried out at 500°C, reducing the billets from 60 mm diameter to 24 mm diameter. The extruded rods were then rod rolled to 6 mm in a series of steps and subsequently drawn into wires, using successively smaller dies, to a minimum diameter of 1 mm without (sample NN) or with (sample AA) three intermediate heat treatments at 450°C. The cold drawing strain η after high temperature extrusion is 6.2, where $\eta=\ln(A_0/A)$ and A_0 and A are the original and final cross-sectional areas, respectively. The reduction in area during cold drawing is 99.2%.

The evaluation of tensile mechanical properties of wires was carried out on a United machine equipped with an nextensometer using specially designed wire grips. All tensile tests were performed at room temperature using a strain rate of 5.5×10^{-4} s^{-1}. The evolution of the microstructure was examined by optical microscope and SEM (scanning electron microscope). The width of Cu matrix between filaments were determined using an image analyzer (Leica Q5001W with Leica Qwin software). Fracture surfaces of the tensile specimens were examined in a SEM (JSM 5410) to characterize fracture behavior. Electrical resistivity measurements were made using a standard four-probe technique.

3. Results and discussion

Fig. 1 shows optical images of the morphology of the Fe dendrites in the as-cast ingot. Fig. 2a,b shows the EDS spectra from Fe dendrite (Fig. 2a) and Cu matrix (Fig. 2b) of Cu–Fe–Co ingot. It is interesting to note from these EDS spectra that Co atoms are mostly observed in the filaments and the Cu matrix is almost free of Co atoms. This result is consistent with the observations that Co in Cu at low temperatures is negligible and Co is completely soluble in Fe [10]. Fig. 3a,b shows the transverse (Fig. 3a) and longitudinal (Fig. 3b) sections of drawn Cu–Fe–Co wires. The ribbon-like morphology of the filaments is clearly evident on the transverse sections (Fig. 3a). On the longitudinal sections (Fig. 3b), the alignment of the filaments with wire axis is readily apparent. The average widths between filaments calculated using an image analyzer were 1.6 μm for Cu–Fe–Co wires.

Fig. 4 shows the variations in hardness with the percentage of drawing reduction in Cu–Fe–Co wires without (sample NN) and with (sample AA) intermediate heat treatments. The micro-vickers hardness was found to increase gradually with the percentage of drawing reduction and the hardness increase rate shoot up beyond 90% reduction. Hardness dropped after intermediate heat treatment and recovered rapidly with further reduction in area as shown in Fig. 4. Although the final micro-vickers hardness was not greatly influenced by intermediate annealing, the wires could be drawn to a long wires following heat treatment at 450°C. Without heat treatment, the maximum wire length after drawing to 1 mm in diameter was about 30 cm.

The ultimate tensile strength (UTS) of Cu–Fe–Co wires with intermediate heat treatments (AA) was observed to be 855 MPa. The UTS of Cu–Fe–Co wires without intermediate heat treatment (NN) were not obtained because wires over 50 cm are needed to wind the wire grips for tensile testing. However, since the micro-vickers hardness of Cu–Fe–Co (NN) are a little larger than that of Cu–Fe–Co (AA) as shown in Fig. 4, the strength of Cu–Fe–Co (NN) are expected to be a little greater than that of Cu–Fe–X (AA). The strengthening in Cu–Fe–Co microcomposites results from the presence of the aligned filaments and correlates with the fineness of the micro-

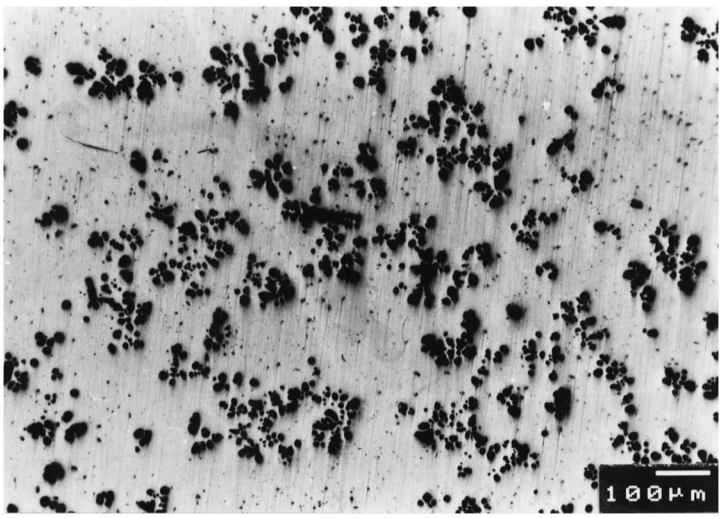

Fig. 1. Cast structures of Cu–9Fe–1.2Co microcomposites.

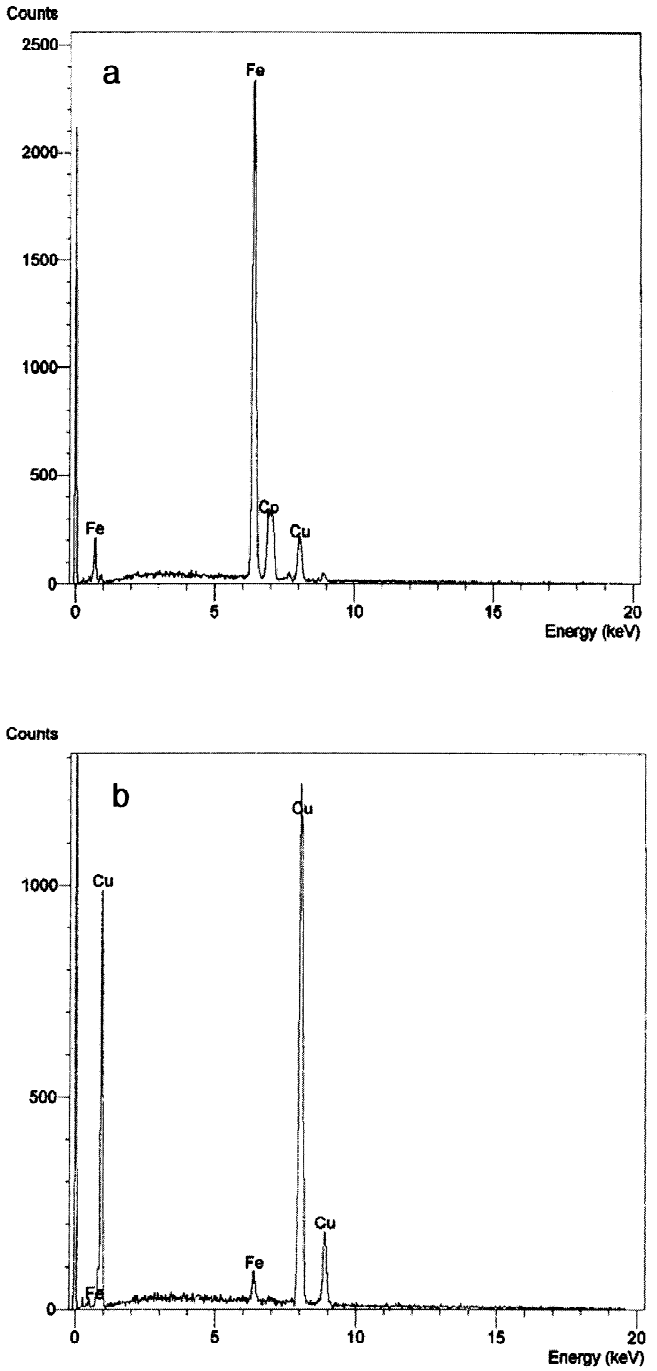

Fig. 2. EDS spectra from Fe dendrite (a) and Cu matrix (b) of Cu–9Fe–1.2Co.

structural scale. Therefore, the strength of Cu–Fe–Co microcomposites can be described by the following Hall–Petch equation:

$$\sigma = \sigma_0 + k\lambda^{-1/2} \quad (1)$$

where σ_0 is the friction stress, k the Hall–Petch coefficient and λ the spacing between filaments. The friction stress may include the lattice friction and precipitation strengthening. The coefficient k was reported to be 1.0 $MN/m^{3/2}$ [11]. In Cu–Fe–Co microcomposites, the friction stress may be assumed to be negligible compared to the high strength of filamentary structure [6]. The predicted strength using Eq. (1) is 789 MPa, which is in reasonably good agreement with the observed strength (855 MPa). The slight difference is associated with the intrinsic friction stress of Cu matrix.

The conductivity of Cu–Fe–Co wires with intermediate heat treatments (AA) were found to be approximately 53.3% IACS, whereas Cu–Fe–Co wires without intermediate heat treatments (NN) showed relatively low conductivity (40.2% IACS). It is interesting to note that the electrical conductivities of wires increased after intermediate heat treatments.

The resistivity of Cu–Fe–X microcomposites can be partitioned into the contribution of four scattering mechanisms [12–14] as follows:

$$\rho_{Cu-Fe-X} = \rho_{pho} + \rho_{dis} + \rho_{int} + \rho_{imp} \quad (2)$$

where ρ_{pho} is the resistivity contribution from phonon scattering, ρ_{dis} is dislocation scattering, ρ_{int} is the interface scattering, and ρ_{imp} is the impurity scattering. Based on detailed TEM studies, Verhoeven et al. [12] suggested that resistivity in heavily drawn Cu base microcomposite wires is mainly due to electron scattering at Cu–Nb interfaces. The observation that the filament spacing, filament thickness, and electrical conductivity decrease in proportion to wire diameter suggests that interface scattering is predominant in Cu–Nb microcomposites [11–13]. Since the microstructure of Cu–Fe–Co microcomposite is similar to that of Cu–Nb microcomposite, the resistivity in heavily drawn Cu–Fe–Comicrocomposite wires is mainly due to electron scattering at Cu–Fe interfaces. However, the electrical conductivity of Cu–Fe microcomposite is generally lower than that of Cu–Nb microcomposites [8,9,13]. The higher resistivity of Cu–Fe wire is suggested to be due to a higher contribution from impurity scattering, ρ_{imp} [8,9,13]. Cu matrix dissolves considerably more Fe than Nb at temperatures above around 250–300°C and Fe has a very large resistivity decrement in Cu [13]. Jerman et al. [13] investigated the temperature dependence of the resistivity in Cu–Fe and found that the resistivity increased dramatically starting at around 500°C due to the large contribution of ρ_{imp}. They [13] also observed that the resistivity of Cu–Fe, after furnace cooling to room temperature, remained significantly high due to a significant amount of dissolved Fe, which did not readily precipitated from solid solution.

The increase of conductivity in Cu–Fe–Co after intermediate heat treatments at 450°C is attributed to the precipitation of Fe and Co atoms which were dissolved during heavy drawing. It is well known that some precipitates dissolve and the solubility of impurities and alloying elements increases in the region of severe deformation

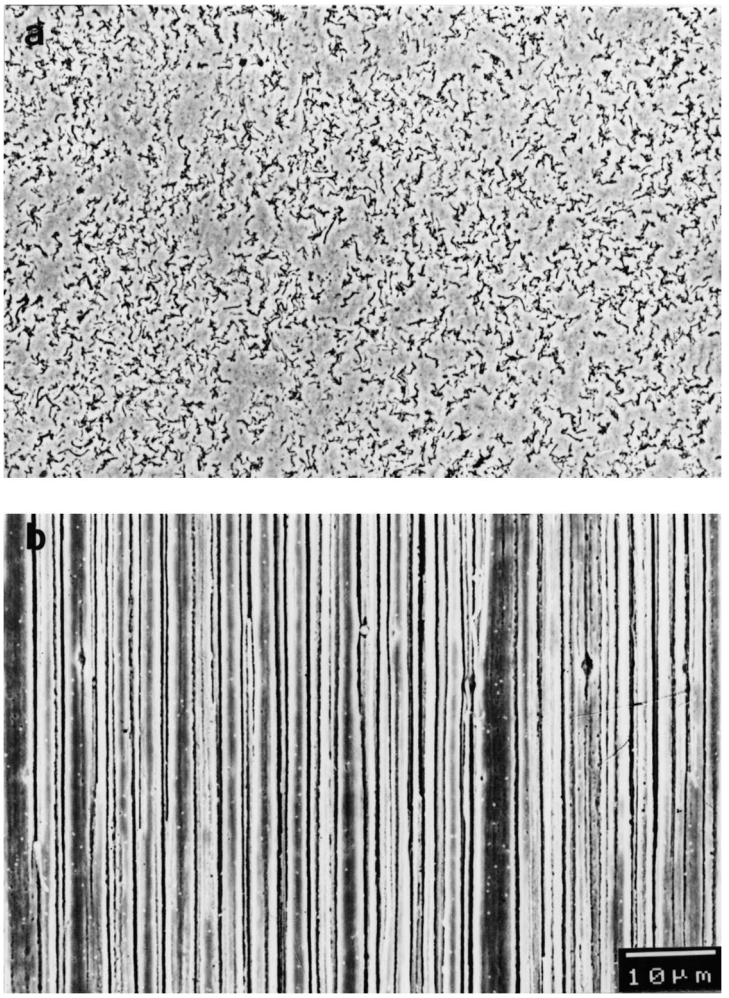

Fig. 3. Microstructures of transverse (a) and longitudinal (b) sections of Cu–9Fe–1.2Co microcomposite wires.

[5,15]. The relatively high solubility of iron in copper at high temperature, coupled with the slow kinetics of iron precipitation at low temperatures make it difficult to achieve the low solubility levels in Cu–Fe microcomposites. The precipitation of impurities and alloying elements during intermediate heat treatments would increase the conductivity due to the reduced impurity scattering [12,13].

In this study, the tensile strength/electrical combination of 855 MPa/53.3% IACS was achieved in Cu–9Fe–1.2Co microcomposite. Verhoeven et al. [9] reported that UTS values of 1000–1200 MPa were obtained at the IACS level of 53% in Cu–20wt.%Fe microcomposites. The relatively lower strength in the present study may be due to the lower volume percentage of Fe filaments and relatively lower drawing ratio. It is also possible that the oxygen content in Cu–9Fe–1.2Co in the present study is higher than that in Cu–20wt.%Fe of Verhoeven et al. [9] since Cu–9Fe–1.2Co was melted in the air. Hodge et al. [16] found that the conductivity of air-melted Cu–25Fe–1.5Cr wire was 40–50% at the strength level of 700–900 MPa. Hong and Hill [17] found that the dendrite structure of Cu–Fe–Co was finer than that of Cu–Fe–Cr. The addition of Cr to Cu–Fe is known to limit the liquid solubility of iron in copper, making it difficult to obtain evenly distributed dendrites [16]. Cobalt is known to reduce the stacking fault energy and grain boundary energy in the Co–Fe system [18], implying that the interphase energy of Fe dendrites may be reduced by the addition of Co. In this case, the nucleation of Fe dendrites is easier with the addition of Co, resulting in the finer dendrite structure [17]. Cu–9Fe–1.2Co has a slightly better strength/conductivity combination than Cu–Fe–Cr alloys [16,17] at similar drawing strain, which may be associated with the finer microstructure.

4. Conclusions

Based upon a study on the strength and conductivity of Cu–Fe–X microcomposite wires, the following conclusions can be drawn.

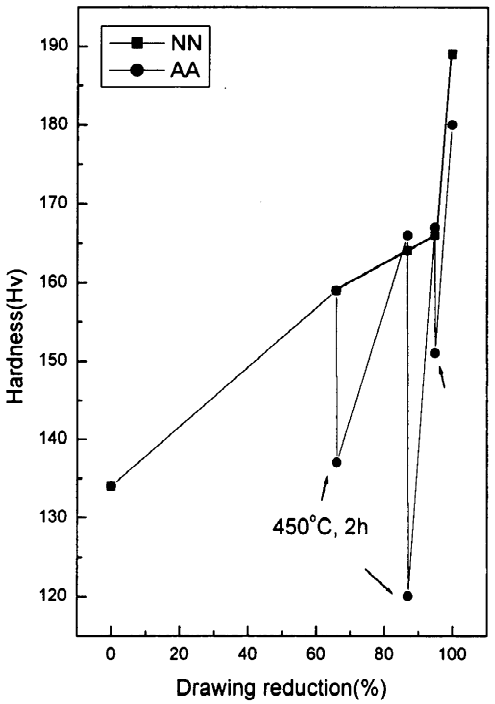

Fig. 4. Variations in hardness with the percentage of drawing reduction in heavily deformed Cu–9Fe–1.2Co microcomposite wires processed by various deformation schedule.

1. The strengthening in Cu–Fe–Co microcomposites results from the presence of the aligned filaments and correlates with the fineness of the microstructural scale. The predicted strength using Hall–Petch equation is 789 MPa, which is in reasonably good agreement with the observed strength (855 MPa).
2. The conductivity of Cu–Fe–Co wires with intermediate heat treatments (AA) were 53.3% IACS, whereas Cu–Fe–Co wires without intermediate heat treatments (NN) showed relatively low conductivity (40.2% IACS). The increase of conductivity after intermediate heat treatments at 450°C is attributed to the precipitation of Fe and Co atoms which were dissolved during heavy deformation processing.

Acknowledgements

The authors acknowledge the support from Kumwon Co. and Korea Science and Engineering Foundation (971-0803-034-2).

References

[1] C. Biselli, D.G. Morris, Acta Mater. 44 (1996) 493.
[2] P.D. Funkenbusch, T.H. Courtney, Acta Metall. 33 (1985) 913.
[3] W.A. Spitzig, A.R. Pelton, F.C. Laabs, Acta Metall. 35 (1987) 2427.
[4] J.D. Verhoeven, L.S. Chumbley, F.C. Laabs, W.A. Spitzig, Acta Metall. 39 (1991) 2825.
[5] S.I. Hong, M.A. Hill, Acta Mater. 46 (1998) 4111.
[6] S.I. Hong, Scripta Mater. 39 (1998) 1685.
[7] J.D. Verhoeven, W.A. Spitzig, L.L. Jones, H.L. Downing, C.L. Trybus, E.D. Gibson, L.S. Chumbly, L.S. Fritzemeier, G.D. Schnittgrund, J. Mater. Eng. 12 (1990) 127.
[8] Y.S. Go, W.A. Spitzig, J. Mater. Sci. 26 (1991) 163.
[9] J.D. Verhoeven, S.C. Chueh, E.D. Gibson, J. Mater. Sci. 24 (1989) 1748.
[10] T. Nishizawa, K. Ishida, in: T.B. Massalski, H. Okamoto, R.R. Subramanian, L. Kacprzak (Eds.), 2nd Edition, Binary Alloy Phase Diagrams, Vol. 2, ASM International, Materials Park, OH, 1990, p. 1181.
[11] W.A. Spitzig, Acta Metall. Mater. 39 (1991) 1085.
[12] J.D. Verhoeven, H.L. Downing, L.S. Chumbly, E.D. Gibson, J. Appl. Phys. 65 (1989) 1293.
[13] G.A. Jerman, I.E. Anderson, J.D. Verhoeven, Metall. Trans. 24A (1993) 35.
[14] S.I. Hong, M.A. Hill, Mater. Sci. Eng. A264 (1999) 151.
[15] S.I. Hong, M.A. Hill, Mater. Sci. Eng. A281 (2000) 189.
[16] W. Hodge, R.A. Happe, B.W. Gonser, Wire Wire Products 26 (1951) 1033.
[17] S.I. Hong, M.A. Hill, unpublished result, Chungnam National University, 2000.
[18] L.E. Murr, in: Interfacial Phenomena in Metals and Alloys, Addison-Wesley, Reading, MA, 1975, p. 145.